



Mechanism of burst feeding in ZL205A casting under mechanical vibration and low pressure

Ru-jia WANG, Shi-ping WU, Wei CHEN

School of Materials Science and Engineering, Harbin Institute of Technology, Harbin 150001, China

Received 20 May 2017; accepted 8 November 2017

Abstract: The burst feeding behavior of ZL205A casting under mechanical vibration and low pressure was investigated by casting experiment and physical model. Experimental results indicated that the burst feeding appeared repeatedly during solidification and left a shrinkage cavity with layered structure under mechanical vibration. The castings with less shrinkage and higher density could be achieved through the vibration. The calculation results of physical model showed that the burst feeding could perform spontaneously under vibration while difficultly without vibration in low-pressure die casting. The obstruction of a casting could be broken and the grains could be rearranged by the vibration. And the obstruction could be carried away due to the inner and outer pressure difference, causing a burst feeding.

Key words: burst feeding; ZL205A alloy; mechanical vibration; low pressure; physical model

1 Introduction

ZL205A is a kind of high-strength casting aluminum alloy widely used in China's aerospace industries for manufacturing of aircraft and spacecraft because of its excellent mechanical properties [1]. However, due to its wide crystallization temperature range, up to 100 °C, and its solidification mode of paste, its casting performance is poor. If the casting process is not properly designed, such casting defects as shrinkage cavity and porosity can be easily caused [2]. In order to enhance the feeding capacity during solidification, a low-pressure casting is used in the production process [3]. However, there is still a large number of shrinkage porosities in large thin-wall cylindrical castings [4]. Through the investigation, it is found that the mechanical vibration can be used to improve the non-homogeneous nucleation of melt [5], break the dendrite [6], increase the filling capacity of metal fluid [7], and greatly improve the comprehensive performance [8]. In this work, the mechanical vibration is introduced into the low-pressure casting, in order to solve the problem of shrinkage cavities of ZL205A casting. The mechanism of feeding in ZL205A casting solidified under mechanical vibration and low pressure is significant.

In 1969, CAMPBELL and FRENG [9] proposed a total of five feeding mechanisms: liquid feeding, mass feeding, interdendritic feeding, burst feeding and solid feeding. Unfortunately, since there is no direct evidence that the burst feeding process exists in the solidification process, this mechanism is still a logical assumption so far. Although the influencing factors of burst feeding is still not clear, the burst feeding concept used to explain some solidification phenomenon is successful and effective [10]. DAHLE and STJOHN [11] designed a shear rheological experiment to determine the starting temperature of burst feeding, dendrites' beginning to lap, and the stopping temperature, the solidus. ZHANG et al [12] and DAHLE et al [13] believed that the mechanical collapse of the dendrite network is possible during the solidification process, depending on the type of alloy and the solidification condition. During the outbreak of dendritic network, the mechanical rearrangement or collapse of grains is a possible way of the feeding behavior during solidification, especially in the paste solidification. WANG [14] found that the shrinkage of ZL205A casting during solidification produces several distinctive vibration, which indirectly proved the existence of burst feeding behavior, and the vibration only occurred in three of seven experimental results, indicating that the burst feeding was accidental

during the static solidification.

In summary, the burst feeding behavior has not been studied at the microscopic level, and the effect of vibration has less been studied on the feeding during solidification under low-pressure casting. Therefore, it is necessary to discuss the mechanism of burst feeding and to verify the effect of vibration on the burst feeding experimentally and theoretically.

2 Experimental

2.1 Experimental principle

The experimental apparatus for mechanical vibration treatment used in this work mainly consists of a resistance furnace, a metal mold, a pressure control system, and a vibration motor with excitation force ranging from 0 to 0.4 kN, as shown in Figs. 1(a)–(c). The structure of casting is shown in Fig. 1(d).

Melt was filled into cavity through the riser under air pressure, and vibration was transmitted to the casting through a medium and metal mold made of 45 steel. The filling speed, rate of pressurization, crystallizing pressure

and other parameters during casting process could be controlled by the pressure control system.

2.2 Experimental program

The composition of ZL205A alloy (mass fraction, %) was as follows: Cu 4.6–5.4, Mn 0.3–0.5, Ti 0.15–0.30, Cr 0.05–0.20, B 0.005–0.05, Cd 0.15–0.24, V 0.05–0.25 and Mg balanced. During the casting procedure, the temperature of the melt, the preheating temperature of the mold, and the vibration time were precisely controlled. Firstly, the ZL205A alloy melt was heated to $(710 \pm 5)^\circ\text{C}$, then the degassing and slag skimming treatments were applied for 3 min approximately, and the melt was held for 5 min. Secondly, the metal mold preheated at $(310 \pm 5)^\circ\text{C}$ was installed in the pressure tank. Then, the pressure control system, with the pressurization rate of 5 kPa/s, crystallizing pressure of 100 kPa and holding time of 5 min, was applied to control the low-pressure casting. Finally, the ZL205A casting was treated by vibration with different amplitudes and frequencies. The experimental program is given in Table 1, including the sample without vibration.

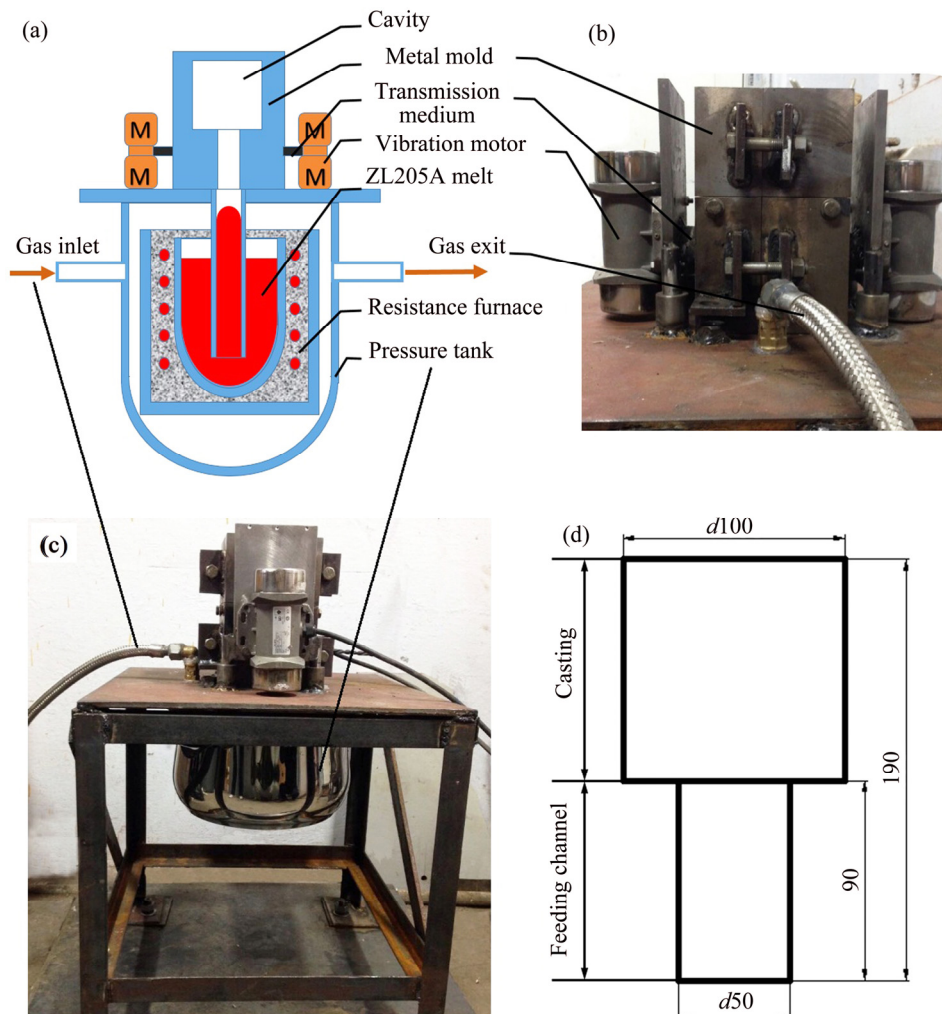


Fig. 1 Experiment apparatus (a–c) and structure of casting (unit: mm) (d)

Table 1 Experimental program

| Sample | Frequency/Hz | Amplitude/mm |
|--------|--------------|--------------|
| A | 0 | 0 |
| B | 5 | 0.8 |
| C | 15 | 0.5 |
| D | 25 | 0.2 |

2.3 Measuring method of shrinkage and density

The shrinkage volume and density of castings were measured by the drainage method. Equations (1) and (2) are used for calculating the shrinkage volume and the density, respectively. The shrinkage distribution was qualitatively described by the macroscopic observation on the section of casting ordered from the most severe level one to the lightest level four.

$$V_p = \frac{G_3 - G_2}{\rho_w g} \quad (1)$$

$$\rho_c = \frac{G_1}{G_1 - G_3} \rho_w \quad (2)$$

where V_p is the shrinkage volume; ρ_c is the density of casting; ρ_w is the density of water; G_1 is the gravity of casting in air; G_2 is the tension measured in water before cutting; G_3 is the tension measured in water after cutting.

3 Results and discussion

3.1 Observation of burst feeding induced by vibration

The low-pressure feeding capacity can be improved by vibration. As shown in Table 2, after the application of vibration, the average mass of additional feeding is 35.1 g, and the average volume of shrinkage cavity is 11.6 cm³. The castings with less shrinkage and higher density could be achieved through the vibration.

Table 2 Castings defects

| Sample | Mass/g | Shrinkage volume/cm ³ | Density/(g·cm ⁻³) | Shrinkage level |
|--------|--------|----------------------------------|-------------------------------|-----------------|
| A | 2800.8 | 15.63 | 2.7967 | 1 |
| B | 2836.8 | 0 | 2.8038 | 2 |
| C | 2831.7 | 18.61 | 2.8188 | 4 |
| D | 2839.2 | 16.26 | 2.8203 | 3 |

As shown in Fig. 2, castings were cut in the axial direction from the center to obtain a cross-sectional view. Layered shrinkage cavity indicated by the arrows were displayed in Sample C and D solidified under vibration, while non-layered shrinkage was shown in sample A without vibration. The shrinkage cavity didn't appear in Sample B. DAHLE and STJOHN [11] conjectured that burst feeding, in some cases, could lead to the

microstructure showing a layered structure or a layered segregation and holes.

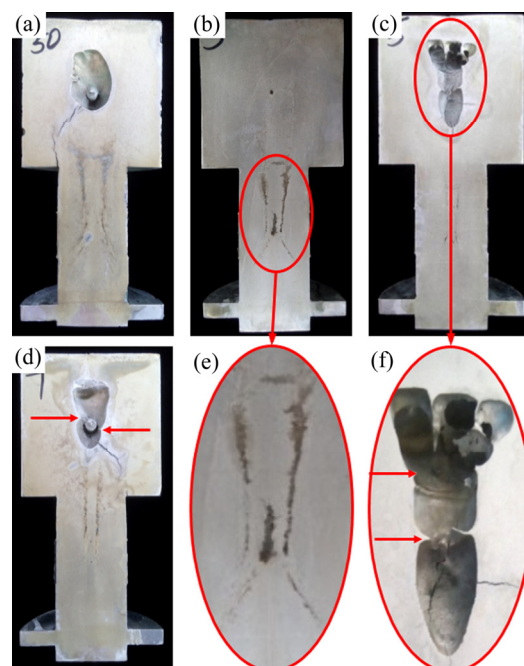


Fig. 2 Sectional view of castings in different solidification conditions: (a) Without vibration; (b) Vibration with frequency of 5 Hz and amplitude of 0.8 mm; (c) Vibration with frequency of 15 Hz and amplitude of 0.5 mm; (d) Vibration with frequency of 25 Hz and amplitude of 0.2 mm; (e) Magnification of channel; (f) Magnification of shrinkage cavity

3.2 Physical model of obstruction in feeding process

As shown in Fig. 3, with the passage size decreasing, the grains of obstruction become more compact and the structure becomes more stable. DAHLE and STJOHN [11] noted that the starting temperature of burst feeding corresponds to a solid fraction about 0.74 for equiaxed grain. Therefore, we focused on the possibility of burst feeding when the passage is obstructed in this form, as shown in Fig. 4, abstracted from the solidification region. It is assumed that the feeding passage has captured so many equiaxed grains to allow only one grain to pass through the throat of feeding passage. For the complex interaction among grains, we assume that the obstruction of standard grains is spherical, and the size of grains is on millimeter level, or even larger. The microscopic interaction among the grains can be ignored compared with the macro-force. Since the grains can be entirely wetted by melt, the friction can be ignored.

3.3 Burst feeding without vibration

Without vibration, the obstruction achieves mechanical equilibrium under the action of gravity, buoyancy and pressure. If we want to break up the obstruction, it is necessary to destroy the captured grains in the passage.

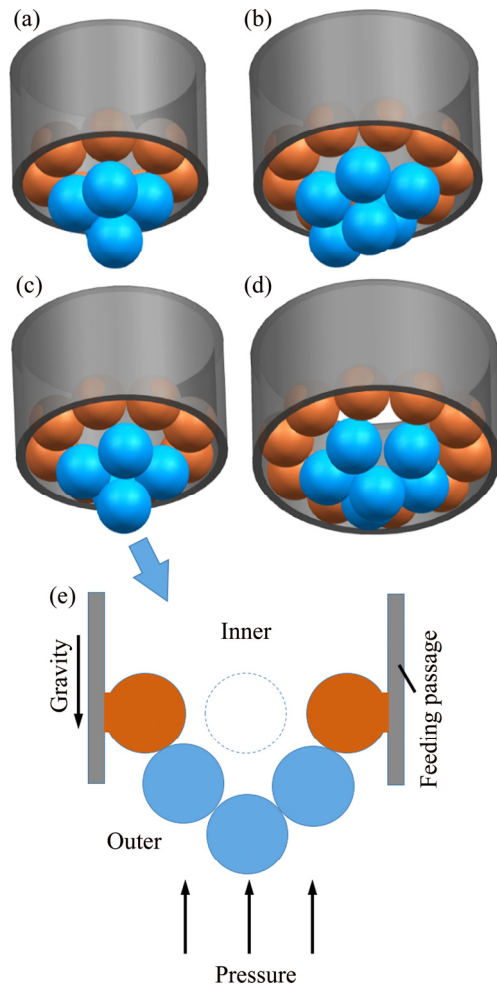


Fig. 3 Structure of obstructions with different sizes of feeding passage (a–d) and section view of obstruction (e)

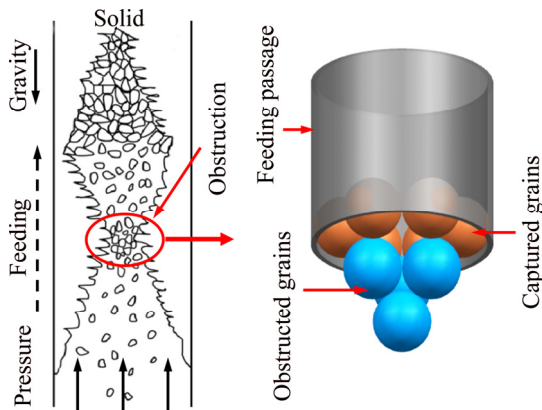


Fig. 4 Physical model abstracted from real obstruction

As shown in Fig. 5, the overall stress of grains in the obstruction keeps balance in the vertical direction:

$$6N \cos \alpha = 4P \quad (3)$$

where N is the interaction force between the captured grains and the obstructed grains; P is the pressure after the grain is offset by the gravity and buoyancy. According to the geometry in Fig. 5, $\cos \alpha = \sqrt{6}/3$.

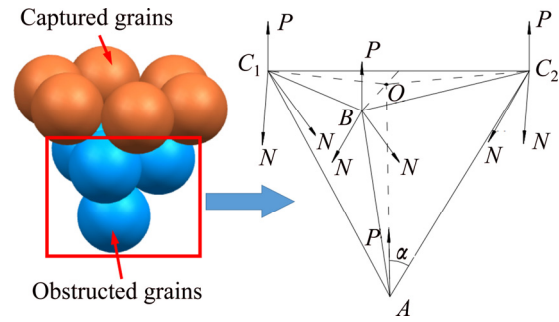


Fig. 5 Stress analysis of obstruction

Considering the captured grains and the obstruction as a whole, the force balance in the vertical direction can be expressed as

$$6nF_{sp} = 10P \quad (4)$$

where n is the number of captured grains along the passage; F_{sp} is the adsorption force of the passage wall with captured grains in the vertical direction.

In the absence of vibration, the obstruction can only be destroyed by increasing the pressure. There are two forms of destruction, breaking the obstructed grains and the captured grains, and releasing the captured grains.

3.3.1 Breaking obstructed grains and captured grains

If both the obstructed and the captured grains are to be destroyed, they both need to undergo plastic deformation:

$$N \cos \alpha / [\pi(R \cos \alpha)^2] \geq e_{sm} \quad (5)$$

where e_{sm} is the yield strength of a grain.

Substituting Eq. (5) into Eq. (3), it yields

$$P \geq \frac{2}{3} \pi R^2 e_{sm} \quad (6)$$

Considering the relationship between the pressure and pressure difference, $P = \Delta P \pi R^2$. Substituting this relationship into Eq. (6), the pressure difference should satisfy

$$\Delta P \geq \frac{2}{3} e_{sm} \quad (7)$$

Because the strength of dendrites is 3–10 MPa [15], to break through the obstruction, according to the Eq. (7), the inner and outer pressure difference of obstruction along the feeding passage should be at least 2–7 MPa.

3.3.2 Releasing captured grains

In order to remove the captured grains, it is necessary to overcome the adhesion force between the passage and grains, F_{spm} , which is equivalent to the shear strength of alloy melt:

$$F_{sp} \geq F_{spm} \quad (8)$$

Substituting Eq. (8) into Eq. (4) and Eq. (3), it yields

$$\Delta P \geq \frac{3nF_{spm}}{5\pi R^2} \quad (9)$$

Assuming that the half volume of captured grains is trapped in the passage because of solidification, the relationship between adhesion force F_{spm} and shear strength τ_{sp} is $F_{spm} = 2\pi R^2 \tau_{sp}$. Substituting this relationship into Eq. (9), the pressure difference should satisfy

$$\Delta P \geq \frac{6n\tau_{sp}}{5} \quad (10)$$

According to Ref. [11], the shear strength of Al–4%Si–4%Cu alloy is about 5–10 kPa. Analyzing Eq. (10), the pressure difference should be at least 6–12 kPa to release captured grains when there is only one layer of captured grains along the feeding passage. However, there are a great number of grains along the passage when it is blocked, causing the pressure difference needed to be large. In the experiment of WANG [14], the height of crucible was 260 mm, approximately equal to the required pressure, so the vibration produced by burst feeding was observed occasionally.

In summary, under the non-vibration condition, the formation of burst feeding is mainly due to the increasing of inner and outer pressure difference, which is difficult to achieve in the normal casting method.

3.4 Burst feeding with vibration

Vibration could change the structure of mixtures [16]. If the potential energy of the system is increased under the effect of vibration, according to the principle of minimum potential energy, the structure before vibration is stable, and the structure should return to the original equilibrium state after the vibration is removed. By contrast, the structure would change continually if the potential energy is reduced after vibration. Therefore, the potential energy of obstruction system is calculated to investigate the effect of vibration on burst feeding.

As shown in Fig. 6, the potential energy of the whole system can be given by

$$W = (h_A + h_B + h_{C_1} + h_{C_2})P \quad (11)$$

The zero-potential energy surface is defined as plane $D_1E_1F_1F_2E_2D_2$. According to the geometrical relationship shown in Fig. 4, the potential energy of the whole system can be expressed as

$$W = \frac{2\sqrt{6}}{3}RP(\cos\theta + 2\sqrt{2}\sin\beta + \sqrt{2}\sin\alpha) \quad (12)$$

where α , β and θ are not isolated. Due to the pressure difference, the captured grains always have the tangential relationship with the obstructed grains. The relationship among α , β and θ can be expressed as

$$\begin{cases} (\sin\beta - \sin\alpha)^2 + (1 - \cos\alpha)^2 + (1 - \cos\beta)^2 = \frac{4}{3} \\ \frac{2\sqrt{3}(\sin\beta - \sin\alpha)}{5(1 - \cos\beta)} = \sin\theta, \quad \alpha \in \left[0, \arcsin\left(\frac{2\sqrt{2}}{3}\right)\right] \end{cases} \quad (13)$$

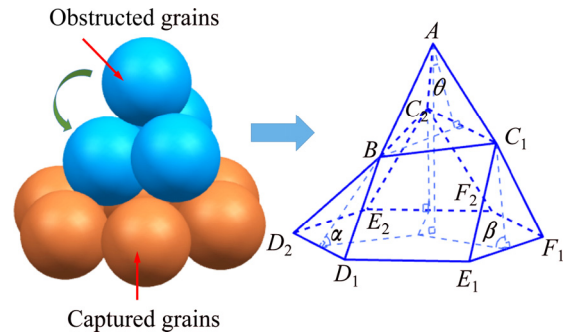


Fig. 6 Structure of obstruction with vibration

As shown in Fig. 7 constructed by Matlab package due to Eqs. (12) and (13), with the decreasing of α , the potential energy of obstruction reduces gradually, i.e., the smaller the α is, corresponding to the changed structure of obstruction, the more stable the structure is. With vibration applied to the obstruction system, the obstruction gradually collapses, as presented in Fig. 7. The calculation indicates that the obstruction in the feeding passage could collapse easily with the influence of vibration and low pressure.

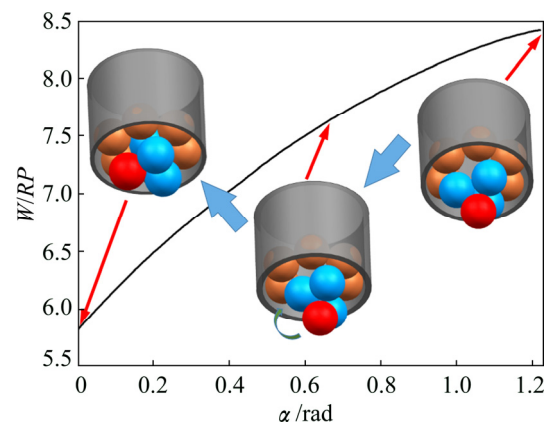


Fig. 7 Relationship of potential energy of obstruction with α

3.5 Burst feeding induced by vibration in castings

As shown in Fig. 8(a), when grains competed through the narrow passage, they restricted each other and clogged the throat easily. With the influence of vibration, grains in the obstruction could be rearranged continuously to reduce the total potential energy according to the calculations above, causing the

movement of grains, as shown in Fig. 8(b). When the equilibrium of block structure was broken, the feeding passage would be suddenly opened to form a burst feeding, as shown in Fig. 8(c). However, with the increasing of solid fraction in the melt, the passage would be blocked consequentially by the flow of grains once again, leading to the stop of burst feeding. The feeding passage would repeat the “blocked–open–blocked” process shown in Fig. 8, and the burst feeding may occur in each cycle, until the vibration was important.

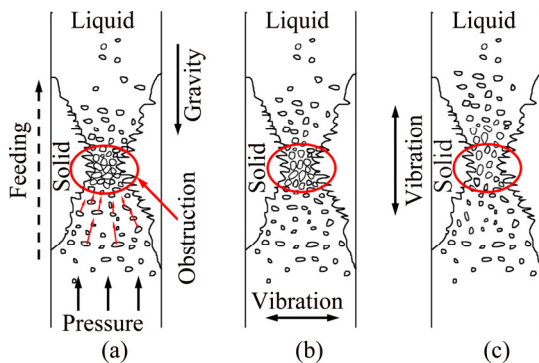


Fig. 8 Burst feeding process: (a) Feeding channel obstructed; (b) Grains of obstruction rearranged; (c) Feeding passage opened and burst feeding occurring

Since the passage repeated “blocked–open–blocked” process constantly, castings would leave layered structure under vibration [11]. Because of the obstruction of feeding passage, shrinkage of casting during solidification would lead to a great negative pressure in the center of casting, leaving a shrinkage cavity, as shown in Figs. 9(a) and (b). Under the impact of vibration, the obstruction was opened, and then a large amount of slurry metal burst into the casting. However, the molten metal filled-in was not enough to fill the cavity completely. With the decreasing of negative

pressure, the feeding process became more and more difficult until the filling stopped. Since the metal film was lifted up suddenly, the edges of the film were tilted upwards, as shown in Fig. 9(c). Due to the shrinkage of solidification, the film separated from the liquid metal and formed the first film, as shown in Fig. 9(d). The layered structure was formed by the intermittent burst feeding under the dual role of pressure difference and vibration. The inner and outer pressure difference of feeding passage is a prerequisite for burst feeding. It was unable to open the obstruction if the filling pressure was extremely weak, even though the grains of obstruction could rearrange under vibration.

The rearrangement of grains of obstruction is a possible way to form the burst feeding under the effect of mechanical vibration. There are many other effects of vibration to promote the forming of burst feeding.

(1) Vibration can reduce the apparent viscosity and flow resistance of melt. The semi-solid slurry of Al–Cu alloy is a pseudoplastic fluid [17] and its apparent viscosity decreases with the increasing of shear rate [18]. Vibration causes the relative motion among the grains, and increases the shear rate between the parts of melt, which is beneficial to reducing the apparent viscosity of melt.

(2) Vibration increases the flow of molten metal and promotes refinement. Although the structure of ZL205A alloy during solidification is composed of equiaxed crystals, the strong forced convection will promote the formation of “crystal rain” [19], and increase the nucleation rate.

(3) Vibration can weaken or even break the connection among grains of slurry, reducing the flocculation among them. It could reduce the head loss during slurry transport. However, it requires appropriate vibration parameters, since vibration has not only the role of fragmentation, but also the action on coagulation [20].

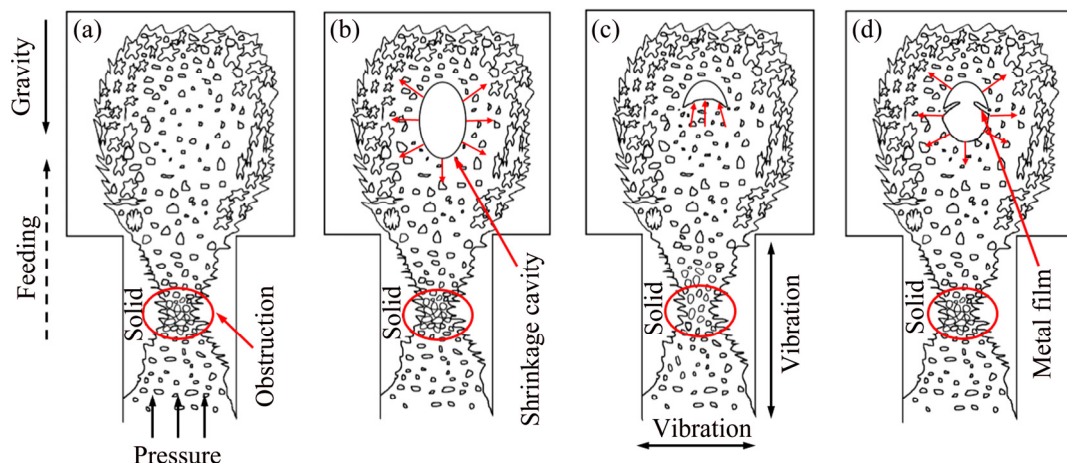


Fig. 9 Formation of layered cavity: (a) Feeding passage obstructed; (b) Forming a shrinkage cavity; (c) Forming burst feeding; (d) Forming thin film of layered structure

4 Conclusions

1) The obstruction of ZL205A alloy during solidification in low-pressure die casting is unstable. It could be destroyed by mechanical vibration and a burst feeding would form to achieve castings with less shrinkage and higher density.

2) The burst feeding appears repeatedly during solidification and leaves a shrinkage cavity with layered structure under mechanical vibration. The layered structure of shrinkage cavity can be regarded as the proofs of the existence of burst feeding. The difference of layers in number and size indicates the contingency of burst feeding.

3) In the low-pressure die casting with mechanical vibration, the vibration is an inducement of burst feeding, and the inner and outer pressure difference along the feeding passage is a prerequisite for burst feeding.

References

- [1] MI Guo-fa, WANG Kuang-fei, GONG Hai-jun, WANG Hong-wei, ZENG Song-yan. Microstructure and properties of ZL205 alloy [J]. China Foundry, 2008, 5(1): 24–27.
- [2] WANG Ye, WU Shi-ping, NIU Lian-jie, XUE Xiang, ZHANG Jian-bing, XIAO Wen-feng. Optimization of low-pressure die casting process parameters for reduction of shrinkage porosity in ZL205A alloy casting using Taguchi method [J]. Journal of Engineering Manufacture, 2014, 228(11): 1508–1514.
- [3] WANG Ye, WU Shi-ping, XUE Xiang, CHEN Rui-run, ZHANG Jian-bing, XIAO Wen-feng. Formation mechanism and criterion of linear segregation in ZL205A alloy [J]. Transactions of Nonferrous Metals Society of China, 2014, 24(11): 3632–3638.
- [4] LI Yu-sheng, ZHAI Hu, FENG Zhi-jun, QU Xua-hui. Formation law and criterion of nebulous macroscopic segregation in ZL205A alloy castings [J]. China Foundry, 2008, 5(1): 20–23.
- [5] KHALIFA W, TSUNEKAWA Y. Production of grain-refined AC7A Al–Mg alloy via solidification in ultrasonic field [J]. Transactions of Nonferrous Metals Society of China, 2016, 26(4): 930–937.
- [6] GUO Hong-min, ZHANG Ai-sheng, YANG Xiang-jie, YAN Ming-ming. Grain refinement of Al–5%Cu aluminum alloy under mechanical vibration using meltable vibrating probe [J]. Transactions of Nonferrous Metals Society of China, 2014, 24(8): 2489–2496.
- [7] KOCATEPE K. Effect of low frequency vibration on porosity of LM25 and LM6 alloys [J]. Materials & Design, 2007, 28(6): 1767–1775.
- [8] XUE Han-song, XING Zhi-hui, ZHANG Wei-na, YANG Gang, PAN Fu-sheng. Effects of ultrasonic treatment on microstructure and mechanical properties of Mg–6Zn–0.5Y–2Sn alloy [J]. Transactions of Nonferrous Metals Society of China, 2016, 26(7): 1826–1834.
- [9] CAMPBELL J, FRENG O. Castings [M]. 2nd ed. Bodmin: MPG Books Ltd, 2003.
- [10] DAHLE A K, ARNBERG L, APELIAN D. Burst feeding and its role in porosity formation during solidification of aluminum foundry alloys [C]//101st Casting Congress. Seattle: AFS Transactions, 1997: 963–970.
- [11] DAHLE A K, STJOHN D H. Rheological behaviour of the mushy zone and its effect on the formation of casting defects during solidification [J]. Acta Materialia, 1998, 47(1): 31–41.
- [12] ZHANG Y F, ZHOU C, ZHANG Z H, GAO G M, ZHANG J. Rheological research of partially-solidified dendritic Sn–14.8wt%Pb alloy by two backward extrusion methods [J]. Materials Science & Technology, 2016, 32(10): 1004–1015.
- [13] DAHLE A K, JOHN D H S, THEVIK H J, ARNBERG L. Modeling the fluid-flow-induced stress and collapse in a dendritic network [J]. Metallurgical & Materials Transactions B, 1999, 30(2): 287–293.
- [14] WANG Ye. Formation mechanism of the macrosegregation and feeding behavior in ZL205A cylindrical castings by low pressure die casting process [D]. Harbin: Harbin Institute of Technology, 2015. (in Chinese)
- [15] XING Shu-ming, CHEN Wei-shi, MA Jing, LI Ya-min, HU Han-qi. Crystal detachment in stirring condition [J]. Journal of Hebei University of Science & Technology, 1999, 20(3): 41–45. (in Chinese)
- [16] LIANG Xuan-wen, HOU Zhao-guo, LÜ Zhen, YANG Lei, SHI Qing-fan, LI Liang-sheng, SUN Gang. Cycle of segregation patterns in vertically vibrated binary granular mixtures [J]. Acta Physica Sinica, 2008, 57(4): 2300–2305. (in Chinese)
- [17] SALLEH M S, OMAR M Z, SYARIF J, ABDULRAZAQ M N. An overview of semisolid processing of aluminium alloys [J]. ISRN Materials Science, 2013, 2013(5): 1–9.
- [18] BLANCO A, AZPILGAIN Z, LOZARES J, KAPRANOS P, HURTADO I. Rheological characterization of A201 aluminum alloy [J]. Transactions of Nonferrous Metals Society of China, 2010, 20(9): 1638–1642.
- [19] WANG X, GUAN R, GUO N, Z. ZHAO Z, ZHANG Y, SU N. Metal solidification–nucleation–rate model under coupling effects of shearing flow and vibration [J]. Materials Science & Technology, 2016, 32(2): 154–163.
- [20] ARAI H, NAKAMURA Y, SHIMASAKI S I, TANIGUCHI S. Theoretical model on heterocoagulation of inclusion in molten steel and its experimental verification. Part II: Cold model experiment [J]. Tetsu-to-Hagane, 2015, 101(2): 139–147.

ZL205A 合金铸件在机械振动和低压条件下的爆发式补缩机制

王汝佳, 吴士平, 陈伟

哈尔滨工业大学 材料科学与工程学院, 哈尔滨 150001

摘要: 采用浇注实验和物理模型研究 ZL205A 合金铸件在机械振动和低压条件下的爆发式补缩机制。实验结果表明, 在机械振动条件下, 爆发式补缩会多次出现, 并使铸件中的缩孔呈层状分布。施加机械振动后, 铸件的疏松减小、密度增大。物理模型计算表明, 低压铸造中, 施加机械振动会促使爆发式补缩自发进行; 而在静态下凝固, 爆发式补缩很难出现。振动可以破碎铸件中的堵塞部位, 并使堵塞部位中的晶粒重排, 在阻塞部位的内外压差的作用下, 阻塞发生移动清除, 产生爆发式补缩。

关键词: 爆发式补缩; ZL205A 合金; 机械振动; 低压; 物理模型

(Edited by Bing YANG)